Catal Lett (2008) 125:209–214
DOI 10.1007/s10562-008-9577-3

FTIR Characterization of Fe^{3+}–OH Groups in Fe–H–BEA Zeolite: Interaction with CO and NO

Radoslav Kefirov · Elena Ivanova · Konstantin Hadjiivanov · Stanislaw Dzwigaj · Michel Che

Received: 24 April 2008 / Accepted: 7 July 2008 / Published online: 23 July 2008

Abstract Fe^{3+}–OH groups of a Fe–H–BEA sample prepared by conventional ion-exchange method are characterized by an IR band at 3686–3684 cm^{-1}. They exhibit a weak acidity: upon low-temperature CO adsorption the O–H stretching modes are blue shifted by 100 cm^{-1} and the respective carbonyl adducts are observed at 2158 cm^{-1}. The Fe^{3+}–OH groups are reduced at room temperature by NO to form Fe^{2+}–NO species and NO^+ groups in cationic positions. Desorption of pre-adsorbed NO at temperatures above 373 K regenerates the Fe^{3+}–OH groups. The relation of the Fe^{3+}–OH species to the so-called α-oxygen is discussed.

Keywords Adsorption · BEA zeolite · CO · FTIR spectroscopy · NO · Iron

1 Introduction

Fe-containing zeolites are reported to be effective catalysts in various reactions such as selective catalytic reduction of nitrogen oxides with hydrocarbons [1–3], simultaneous reduction of NO and N_2O by NH_3 [4], selective catalytic reduction of NO by ethanol [5, 6], N_2O decomposition [7, 8] and hydroxylation of benzene with N_2O [9–13]. The redox chemistry of iron is thought to be decisive for these processes. Moreover, it has been shown that these different processes, in particular the two latter ones, require different active sites [12, 13]. A strong correlation has been identified between the rate of N_2O decomposition and the presence of polynuclear Fe species stabilized by extra-framework Al formed as result of high-temperature treatment of Fe-containing ZSM-5. In contrast, it is evidenced that the mononuclear Fe species are active in the selective hydroxylation of benzene to phenol. Indeed, Li et al. [13] have shown that the rate of phenol formation decreases strongly with the increase of iron loading.

Many studies have discussed the nature of the active oxygen species (the so-called α-oxygen) in iron-containing zeolites [4, 9–11, 14, 15]. Different suggestions have been made in the literature: atomic oxygen [4, 9, 10], oxygen anion radicals [15, 16] and/or Fe^{4+}=O groups [14], have been proposed as active species of N_2O decomposition and/or hydroxylation of benzene with N_2O. It is well established that α-oxygen is produced by interaction of reduced samples with N_2O [17]. On the other hand, recent reports showed that iron-hydroxyl groups are formed after interaction of Fe-zeolites with N_2O, suggesting that these hydroxyls might be related to the active oxygen species.

Very recently, Panov et al. [18] elegantly demonstrated the relationship between oxygen anion radicals (α-oxygen) and Fe^{3+}–OH groups in Fe-ZSM-5 zeolite. They proposed the following reaction:

$$2\left(Fe^{3+}{-}O^{-}\right) + H_2O \rightarrow 2\left(Fe^{3+}{-}OH^{-}\right) + \frac{1}{2}\,O_2 \qquad (1)$$

It is also pointed out that the OH groups are less reactive than the O^- species. However, as a rule, the catalytic

---

R. Kefirov · E. Ivanova · K. Hadjiivanov (✉)
Institute of General and Inorganic Chemistry,
Bulgarian Academy of Sciences, Sofia 1113, Bulgaria
e-mail: kih@svr.igic.bas.bg

S. Dzwigaj (✉) · M. Che
Laboratoire de Réactivité de Surface, UMR 7609 – CNRS,
Université Pierre et Marie Curie – Paris 6, 4 Place Jussieu,
75252 Paris, Cedex 05, France
e-mail: dzwigaj@ccr.jussieu.fr

M. Che
Institut Universitaire de France, Paris, France

reactions are usually performed in presence of water which shows that the detailed characterization of the Fe^{3+}–OH groups is of great importance.

The aim of this work is to characterize Fe^{3+}–OH groups in a Fe–H–BEA zeolite and to obtain information about their redox chemistry, in particular towards NO.

2 Experimental

2.1 Materials

A tetraethylammonium BEA (TEABEA) zeolite is provided by RIPP (China). A portion of it is calcined (15 h, 823 K, in air) to obtain organic-free H-BEA (Si/Al = 11) [19, 20]. An iron-containing sample is prepared by conventional ion-exchange in air at 343 K for 3 h using a 2×10^{-3} mol L^{-1} aqueous solution of $Fe(NO_3)_2 \cdot 2.5\ H_2O$ (pH = 2.5). This exchange procedure is repeated two times. The suspension is then filtered and the solid obtained washed with distilled water. This sample is dried in air at 353 K for 24 h and referred to as Fe–H–BEA. According to chemical analysis, it contains 2.1 wt% of iron.

2.2 Techniques

Chemical analysis of the samples is performed with inductively coupled plasma atom emission spectroscopy at the CNRS Centre of Chemical Analysis (Vernaison, France).

FTIR spectra are recorded on a Nicolet Avatar 360 spectrometer accumulating 128 scans for 224 s at a spectral resolution of 2 cm^{-1}. Self-supporting pellets (ca 10 mg cm^{-2}) are prepared from the sample powders and treated directly in a custom-made IR cell allowing measurements at ambient and low temperatures. The cell is connected to a vacuum-adsorption apparatus allowing a residual pressure below 10^{-3} Pa. Prior to adsorption, the samples are activated by treatment first in oxygen (13.3 kPa) for 1 h at 673 K and then outgassing for 1 h at the same temperature.

Carbon monoxide (>99.997 purity) is supplied by Linde AG. Nitrogen monoxide is provided by Messer Griesheim GmbH with a purity >99.0%. Before adsorption, CO is passed through a liquid nitrogen trap, while NO is additionally purified by fraction distillation.

3 Results and Discussion

3.1 Background IR Spectra

The IR spectrum of Fe–H–BEA sample after outgassing at 673 K contains, in the OH stretching region, bands with maxima at 3744, 3737, 3686 and 3608 cm^{-1} (Fig. 1, spectrum a). In addition, a weak shoulder at 3663 cm^{-1} and a broad absorbance centered at around 3530 cm^{-1} are also observed.

Cooling the sample to 100 K leads to some changes in the OH region. The band at 3737 cm^{-1} is now observed as a shoulder and the 3608 cm^{-1} band is shifted to 3612 cm^{-1} (Fig. 1, spectrum b).

It should be noted that prolonged outgassing at 673 K leads to practical disappearance of the band at 3686 cm^{-1} (Fig. 1, spectrum c). This band is not observed either with a hydrogen reduced sample (Fig. 1, spectrum d).

The bands at 3744–3735 cm^{-1} and those at 3663, 3608 and 3530 cm^{-1} are also detected with the parent zeolite. According to the literature [21–24], the band at 3744 cm^{-1} corresponds to external silanols, and that at 3737 cm^{-1}, to internal silanols. The broad feature at 3530 cm^{-1} corresponds to hydrogen-bonded SiOH groups located in hydroxyl nests or framework-defect sites [23]. The band at 3608 cm^{-1} arises from the zeolite acidic Al–O(H)–Si hydroxyls [21–24]. Finally, the 3663 cm^{-1} band corresponds to Al–OH groups [21–24].

The band at 3686 cm^{-1} is absent from the spectrum of the iron-free H–BEA zeolite and is therefore assigned to Fe^{3+}–OH species. A similar band (3683–3670 cm^{-1}) has already been observed by other authors [7, 17, 25, 26], with Fe containing BEA zeolite. It has been reported that the band disappears after H_2-reduction, but appears again when

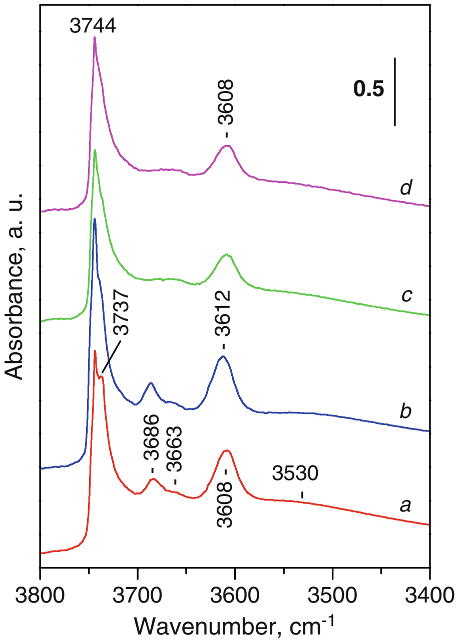

Fig. 1 FTIR spectra (OH stretching region) of Fe–H–BEA zeolite prepared by ion exchange: (a) sample outgassing at 673 K, (b) after cooling to 100 K, (c) after additional prolonged outgassing at 673 K and (d) after reduction with hydrogen at 673 K

the reduced sample is treated with O_2 or N_2O. In what follows, we shall mainly concentrate on this band.

3.2 Low-temperature CO Adsorption on Fe–H–BEA

Low-temperature CO adsorption experiments are designed mainly to study the Brønsted acidity of the Fe^{3+}–OH groups as well as to obtain information on the Lewis acidity of the cationic iron species.

Interaction of CO with OH groups in zeolites is well documented [22, 24, 25]. Due to H-bonding, CO induces a broadening and a red shift of the OH bands. For higher the OH acidity, the larger the shift of the OH modes and the higher the carbonyl frequency is observed.

Introduction of CO (730 Pa equilibrium pressure) to the sample at 100 K leads to the appearance of two principal carbonyl bands, at 2190 and 2175 cm^{-1} (Fig. 2, spectrum a). Two very weak bands are seen at 2231 and 2220 cm^{-1}. In addition, shoulders at 2157, 2143 and 2133 cm^{-1} are detected. The second derivative of the spectrum reveals also shoulders at 2165 and 2154 cm^{-1}.

The bands at 2231 and 2220 cm^{-1} are due to Al^{3+}–CO species [27]. All bands in the range 2175–2155 cm^{-1} correspond to different OH–CO adducts, and these at 2143 and 2133 cm^{-1}, to weakly (physically) adsorbed CO [27]. The band at 2190 cm^{-1} is assigned to Fe^{2+}–CO complexes [25, 28–30]. The position of this band is typical of carbonyls of Fe^{2+} ions exchanged in zeolites [28–30] since Fe^{2+}–CO complexes produced with oxide supported iron [31, 32] or with small Fe_2O_3 clusters in zeolites [33] are observed at lower frequencies. Thus, the results indicate that iron ions in our sample are in cationic positions.

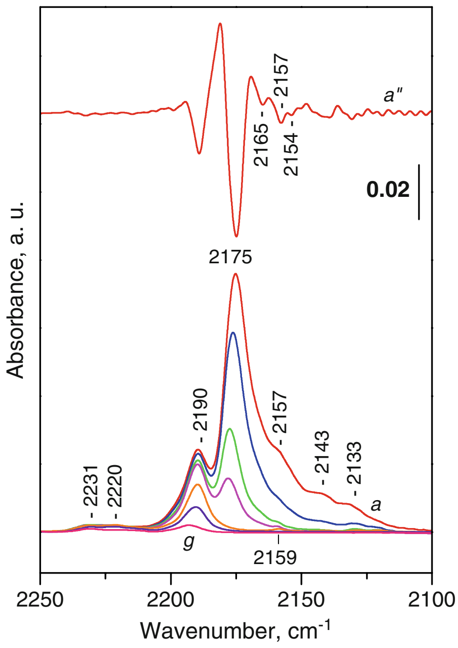

Fig. 2 FTIR spectra (carbonyl stretching region) of CO adsorbed at 100 K on Fe–H–BEA zeolite: (a) equilibrium pressure of 730 Pa CO and (b–e) development of the spectra under outgassing at 100 K and (f, g) at increasing temperatures. The second derivative of spectrum *a* is given in *a''*. The spectra are background corrected

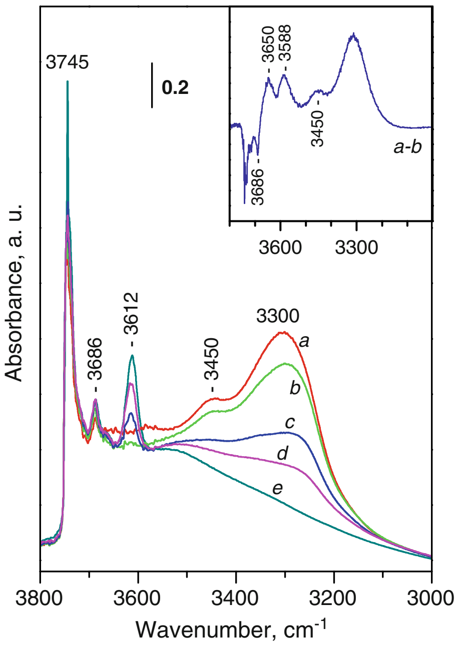

Fig. 3 FTIR spectra (OH stretching region) of CO adsorbed at 100 K on Fe–H–BEA zeolite: (a) equilibrium pressure of 730 Pa CO and (b–e) development of the spectra under outgassing at 100 K. The difference spectrum (a, b) is shown in the inset

Upon decrease of the CO equilibrium pressure and outgassing (Fig. 2, spectra b–g) all bands decrease in intensity to finally disappear, the stability generally increasing with the wavenumber.

We now consider the changes in the O–H stretching region. Upon introduction of CO, the OH bands are eroded and that at 3612 cm^{-1} vanishes (Fig. 3, spectrum a). New, more intense bands at lower frequencies develop at their expense. Analysis of the spectra shows that the bridging hydroxyls are shifted by 312 cm^{-1} (from 3612 to 3300 cm^{-1}) and the associated CO band is at 2175 cm^{-1} (Fig. 2). The Al–OH groups (3662 cm^{-1}) are shifted by 212 cm^{-1} to 3450 cm^{-1} and the corresponding carbonyls are observed at 2165 cm^{-1} (Fig. 2). To measure more accurately the shift of the weakly acidic hydroxyls, we analyzed the difference between two spectra in which the bands at 3612 and 3663 cm^{-1} remained highly perturbed, but the perturbation of the weakly acidic groups strongly differed (see Fig. 3, inset). Two bands, at 3650 and 3588 cm^{-1} are well seen. According to literature data [24, 25], the CO-induced shift of Si–OH groups is ca. 90 cm^{-1}, i.e., a band around 3655 cm^{-1} should correspond to perturbed silanol groups. In the difference spectra, we detect a band at 3650 cm^{-1} (note that the position is not accurate because of the superimposition with the negative band at 3686 cm^{-1}). The corresponding CO vibrations at 2154 cm^{-1} coincide well with literature data [24, 25].

The band at 3588 cm^{-1} is attributed to perturbed Fe^{3+}–OH groups. Therefore, the CO induced shift of the original Fe^{3+}–OH band (3686 cm^{-1}) is 98 cm^{-1}. In agreement with this interpretation, we assign the CO band at 2157 cm^{-1} to Fe^{3+}–OH···CO interaction.

The results suggest an acidity of the Fe^{3+}–OH groups slightly higher than the acidity of the Si–OH groups and similar to that of Zr–OH and Ti–OH groups [27]. Indeed, the band at 3686 cm^{-1} only slightly decreases in intensity upon introduction of CO to the sample, which confirms its weak acidity. To the best of our knowledge, this is the first report of the acidity of these Fe^{3+}–OH groups.

3.3 Adsorption of NO on Fe–H–BEA

It is known that, at high equilibrium pressure, NO can easily disproportionate giving N_2O and NO_2, the latter being a strong oxidizer [34]. In order to prevent this reaction, a small dose of NO is initially adsorbed on the sample. This causes appearance of bands at 2252 (vw), 2136 (s), 1966 (vw), 1876 (s), 1632 (w) and 1611 (w) cm^{-1} (Fig. 4, spectrum a). Increasing the equilibrium NO pressure to 700 Pa leads to an increase of intensity of all bands below 2200 cm^{-1} while that of the band at 2252 cm^{-1} declines (Fig. 4, spectrum b). With time, the changes become more pronounced, the bands around 1620 cm^{-1} showing the most important increase (Fig. 4, spectrum c).

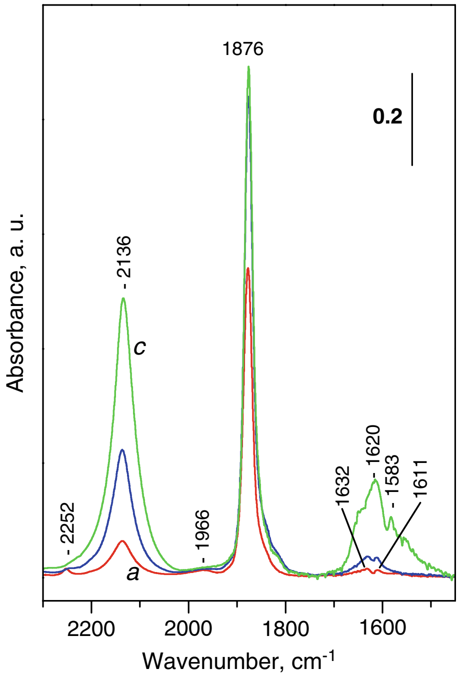

Fig. 4 FTIR spectra (nitrosyl stretching region) of NO adsorbed at 298 K on Fe–H–BEA zeolite: (a) introduction of a small dose of NO to the sample, (b) in the presence of 940 Pa NO and (c) after 1 h. The spectra are background corrected

The weak band at 2252 cm^{-1} is assigned to adsorbed N_2O [35]. The band at 2136 cm^{-1} originates from NO^+ species in cationic positions [31]. The intense band at 1876 cm^{-1} corresponds to Fe^{2+}–NO species [9, 34, 36]. Here again, the position of the band indicates the Fe^{2+} species are in cationic positions. The bands in the 1635–1610 cm^{-1} region are due to adsorbed water (1632 cm^{-1}) and some amount of nitrates.

Consider now the changes in the OH stretching region. The introduction of the small dose of NO leads to a strong decrease in intensity of the Fe^{3+}–OH band at 3684 cm^{-1} (Fig. 5, spectrum b). In addition, the band at 3609 cm^{-1} also decreases but in a less extent. The Si–OH band is only slightly eroded.

In the presence of NO in the gas phase, the Fe^{3+}–OH band at 3684 cm^{-1} disappears and the band of bridged hydroxyls at 3609 cm^{-1} further decreases in intensity (Fig. 5, spectrum c). With time, the band decreases, in parallel with the development of the NO^+ band at 2136 cm^{-1} (Fig. 4, spectrum c).

It has been reported [35] that NO^+ is formed on H-zeolites in the presence of NO and O_2 according to the reactions:

$$2\ NO + \frac{1}{2}\ O_2 + \rightarrow N_2O_3 \qquad (2)$$

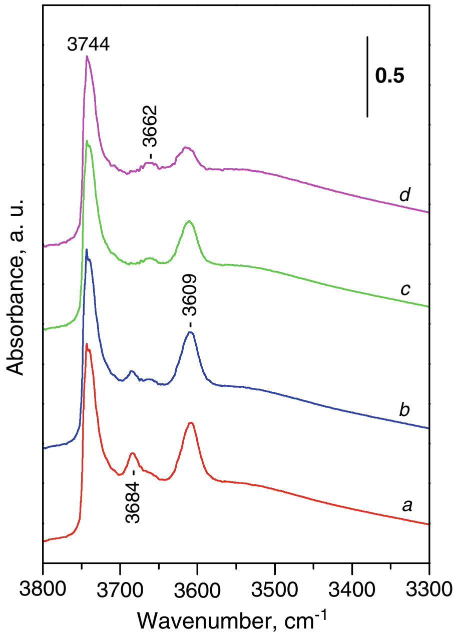

Fig. 5 FTIR spectra (OH stretching region) of (a) Fe–H–BEA zeolite, (b) after introduction of a small dose of NO to the sample, (c) in the presence of 940 Pa NO and (d) after 1 h

$$N_2O_3 + Z{-}OH \rightarrow Z{-}O{-}[NO^+] + HNO_2 \quad (3)$$

$$HNO_2 + Z{-}OH \rightarrow Z{-}O{-}[NO^+] + H_2O \quad (4)$$

where “Z” stands for zeolite.

In our case we have not introduced oxygen to the system, i.e. NO is oxidized by another reagent. The fast intensity decrease of the Fe^{3+}–OH band suggests the following reactions:

$$Fe^{3+}{-}OH^- + NO = Fe^{2+} + HNO_2 \quad (5)$$

$$HNO_2 + Z{-}OH = Z{-}O{-}[NO^+] + H_2O. \quad (6)$$

The fact that NO$^+$ is produced even after the consumption of all Fe^{3+}–OH groups suggests the existence of less reactive oxygen on the sample. However, we cannot rule out the possibility of iron-catalyzed NO disproportionation.

3.4 Desorption of NO preadsorbed on Fe–H–BEA

When the sample with preadsorbed NO is outgassing at room temperature, the NO$^+$ band at 2136 cm^{-1} almost disappears (Fig. 6, spectrum b). This suggests the reverse of reactions (2)-(4). Indeed, the band characterizing bridging hydroxyls (3609 cm^{-1}) is almost restored (Fig. 7, spectrum b). The band of Fe^{2+}–NO species (1876 cm^{-1}) decreases in intensity ca 2 times and a band at 1635 cm^{-1} develops (Fig. 6, spectrum b). The latter is assigned to surface nitrates, and the assignment is strengthened by the appearance of a combination mode at 2614 cm^{-1} (not shown) [37]. Evidently, these species are produced during NO desorption.

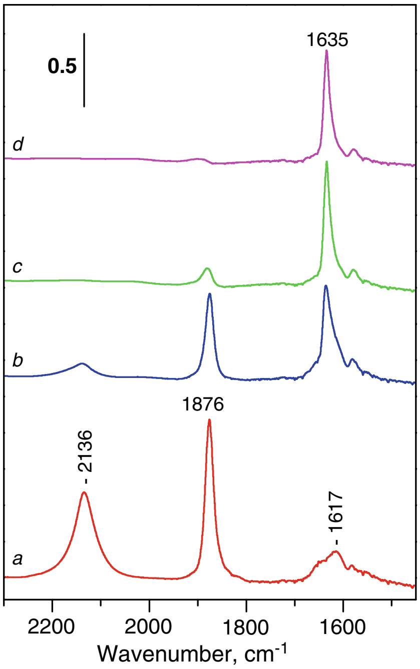

Fig. 6 FTIR spectra (nitrosyl stretching region) of (a) Fe–H–BEA zeolite after adsorption of NO, (b) after outgassing at 298 K, (c) at 373 K and (d) at 473 K. The spectra are background corrected

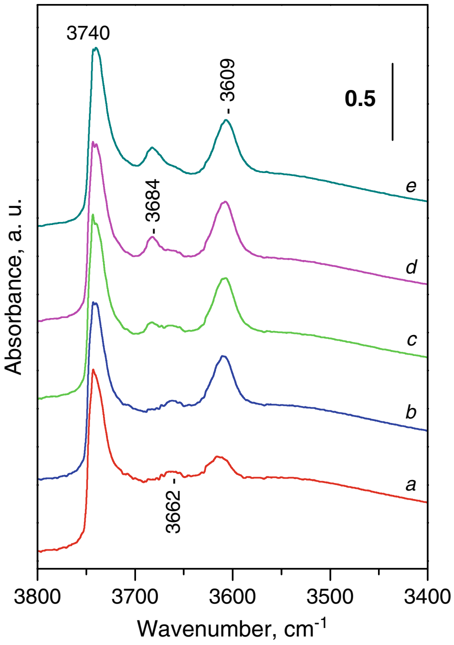

Fig. 7 FTIR spectra (OH stretching region) of (a) Fe–H–BEA zeolite after adsorption of NO, and after outgassing at (b) 298 K, (c) at 373 K, (d) at 473 K and (e) at 673 K

Outgassing at 373 K almost eliminates the Fe^{2+}–NO band (Fig. 6, spectrum c). At the same time, a Fe^{3+}–OH band at 3684 cm^{-1} emerges (Fig. 7, spectrum c). Outgassing at 473 K (Figs. 6 and 7, spectra d) hardly affects the spectra, only the residual nitrosyls at 1876 cm^{-1} are observed. These results indicate that the Fe^{3+}–OH groups are reproduced upon desorption of NO. When the sample is outgassed at 473 K, the band at 3686 cm^{-1} gains some intensity (Fig. 7, spectrum c). Again, the results indicate oxidation of Fe^{2+} by NO$_x$ desorption products.

Finally, we would like to note that the best candidates for the iron sites where the OH groups are formed are the so-called α-Fe ions, the same sites where O$^-$ radicals are formed, as recently shown by Panov et al. [18]. Our results confirm the relationship between α-oxygen and Fe^{3+}–OH species.

4 Conclusions

The aim of this work is to investigate the reactivity of Fe^{3+}–OH groups formed in Fe–H–BEA zeolite prepared by conventional ion-exchange method using aqueous solution of Fe(NO$_3$)$_2$. The Fe^{3+}–OH groups are evidenced by IR band at 3686–3684 cm^{-1}. They exhibit a weak acidity, slightly higher than the acidity of the Si–OH groups and similar to that of Zr–OH and Ti–OH groups. They are reactive toward CO and NO molecules and easy change the oxidation state. Originally they are in the form of Fe^{3+}–OH but are easily reduced by CO and NO to Fe^{2+} with formation of Fe^{2+}–CO and Fe^{2+}–NO complexes evidenced by the IR bands at 2190 and 1876 cm^{-1}, respectively. The Fe^{2+} species can be easily back transformed to Fe^{3+} species by oxidation with NO_x desorption products at temperature between 373 and 673 K. The results show that, although less reactive than α-oxygen, Fe^{3+}–OH groups may play an important role in some catalytic reactions.

Acknowledgments R.K., E.I. and K.H. acknowledge financial support from the EC (project INCO 016414). S.D. gratefully acknowledges CNRS (France) for financial support as Assistant Researcher.

References

1. Feng X, Hall WK (1996) Catal Lett 41:45
2. Kogel M, Monnig R, Schwieger W, Tissler A, Turek T (1999) J Catal 182:470
3. Nobukawa T, Sugawara K, Okumura K, Tomishige K, Kunimori K (2007) Appl Catal B 70:342
4. Coq B, Mauvezin M, Delahay G, Butet J-B, Kieger S (2000) Appl Catal B 27:173
5. Dzwigaj S, Stievano L, Wagner FE, Che M (2007) J Phys Chem Solids 68:1885
6. Janas J, Machej T, Gurgul J, Socha RP, Che M, Dzwigaj S (2007) Appl Catal B 75:239
7. Roy PK, Prins R, Pirngruber GD (2008) Appl Catal B 80:226
8. Kondratenko EV, Perez-Ramirez J (2006) Appl Catal B 64:35
9. Panov GI, Kharitonov AS, Sobolev VI (1993) Appl Catal A 98:1
10. Sobolev VI, Kharitonov AS, Paukshtis YA, Panov GI (1993) J Mol Catal 84:117
11. Wood BR, Reimer JA, Bell AT, Janicke MT, Ott KC (2004) J Catal 224:148
12. Yuranov I, Bulushev DA, Renken A, Kiwi-Minsker L (2007) Appl Catal A 319:128
13. Sun K, Xia H, Feng Z, van Santen R, Hensen E, Li C (2008) J Catal 254:383
14. Jia J, Wen B, Sachtler WMH (2002) J Catal 210:453
15. Chernyavsky VS, Pirutko LV, Uriarte AK, Kharitonova AS, Panov GI (2007) J Catal 245:466
16. Panov GI, Uriarte AK, Rodkin MA, Sobolev VI (1998) Catal Today 41:365
17. Kameoka S, Nobukawa T, Tanaka S, Ito S, Tomishige K, Kunimori K (2003) Phys Chem Chem Phys 5:3328
18. Panov GI, Starokon E, Pirutko L, Paukshtis E, Parmon V (2008) J Catal 254:110
19. Dzwigaj S, Peltre MJ, Massiani P, Davidson A, Che M, Sen T, Sivasanker S (1998) Chem Commun 87
20. Dzwigaj S, Massiani P, Davidson A, Che M (2000) J Mol Catal A 155:169
21. Vimont A, Thibault-Starzyk F, Lavalley JC (2000) J Phys Chem B 104:286
22. Mihaylova A, Hadjiivanov K, Dzwigaj S, Che M (2006) J Phys Chem B 110:19530
23. Jia C, Massiani P, Barthomeuf D (1993) J. Chem Soc Faraday Trans 89:3659
24. Zecchina A, Otero Arean C (1996) Chem Soc Rev 25:187
25. Mauvezin M, Delahay G, Coq B, Kieger S, Jumas JC, Olivier-Fourcade J (2001) J Phys Chem B 105:928
26. Nobukawa T, Yoshida M, Kameoka S, Ito S, Tomishige K, Kunimori K (2004) J Phys Chem B 108:4071
27. Hadjiivanov K, Vayssilov G (2002) Adv Catal 47:307
28. Angell CL, Schaffer PC (1966) J Phys Chem 70:1413
29. Ballivet-Tkatchenko D, Coudurier G (1979) Inorg Chem 18:558
30. Witcherlova B, Kubelkova L, Navakova J, Jiru P (1982) Stud Surf Sci Catal 12:143
31. Bianchi D, Batis-Landousi H, Bennett CO, Pajonk GM, Vergnon P, Teichner SJ (1981) Bull Soc Chim France Part 1 9–10:345
32. Davydov A, Kovillo N (1995) Izv AN SSSR Ser Khim 1946
33. Zecchina A, Geobaldo F, Lamberti C, Bordiga S, Turnes Palomino G, OteroArean C (1996) Catal Lett 42:25
34. Hadjiivanov K (2000) Catal Rev Sci Eng 42:71
35. Hadjiivanov K, Saussey J, Freysz JL, Lavalley JC (1998) Catal Lett 52:103
36. Capek L, Kreibich V, Dedecek J, Grygar T, Wichterlova B, Sobalik Z, Martens JA, Brosius R, Tokarova V (2005) Micropor Mesopor Mater 80:279
37. Hadjiivanov K (2000) Catal Lett 68:157